Optics Communications 443 (2019) 211–215

Contents lists available at ScienceDirect

Optics Communications

journal homepage: www.elsevier.com/locate/optcom

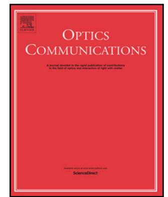

A beam homogenizer for digital micromirror device lithography system based on random freeform microlenses

Zhongyuan Liu [a], Hua Liu [a,b,c,*], Zifeng Lu [a,b], Qiankun Li [a], Jinhuan Li [a,b]

[a] Center for Advanced Optoelectronic Functional Materials Research, and Key Laboratory for UV-Emitting Materials and Technology of Ministry of Education, Northeast Normal University, 5268 Renmin Street, Changchun 130024, China

[b] Demonstration Center for Experimental Physics Education, Northeast Normal University, 5268 Renmin Street, Changchun 130024, China

[c] State Key Laboratory of Applied Optics, Changchun Institute of Optics, Fine Mechanics and Physics, Chinese Academy of Sciences, Changchun 130033, China

ARTICLE INFO

Keywords:
Homogenizer
Microlens array
Freeform surface
DMD lithography system

ABSTRACT

We report a novel beam homogenizer for digital micromirror device lithography system. Such a beam homogenizer contains only one random freeform microlens array (rfMLA). And the rfMLA consists of different freeform microlenses. By the individual design and irregular arrangement of the microlenses, efficient and uniform beam shaping results have been obtained, and the interference patterns in particular are greatly weakened. Compared with traditional beam homogenizer, the energy efficiency has been increased from 62.00% to 69.70%, and the uniformity for incoherent light and coherent light have been improved from 91.93% to 97.60% and from 79.00% to 94.33%, respectively. rfMLA has great potential for enhancing the performance of DMD lithography system and other optical systems, particularly for the homogenization of the beam and the integration of the system.

1. Introduction

Lithography technology, as one core factor in the production of integrated circuits, has influence on the development of information technology. With the continuous improvement of integrated circuits, the requirements for lithography technology have been also increased. In lithography technologies [1–4], digital micromirror device (DMD) lithography technology has been widely used because of mask-less, short response time, and low cost [5–8]. The light source of DMD lithography system is usually semiconductor laser. The beam which comes from the laser tube is coupled to one end of the fiber optic and emitted from the other end. For the following reason, the beam must be homogenized before it arrives at the DMD. One is the inconsistent optical resolution of the lithography pattern resulted from the nonuniform spot on the DMD [9], the other is the Gaussian intensity distribution of the beam emitted from the fiber optic.

In many beam homogenizers [10–13], microlenses array (MLA) is a common beam homogenizer. A traditional MLA beam homogenizer which is composed of a Fourier lens and two identical regular MLA is often called tandem microlens array (tMLA). There are some disadvantages when tMLA apply to DMD lithography system. (i) Due to its excessive number and volume of the components, it is difficult to integrate; (ii) because DMD is in the direction not perpendicular to the optical axis of the beam homogenizer, the uniformity is poor; (iii) the interference patterns on the DMD are obvious and regular because of the periodic structure of tMLA and the coherence of the laser. Rotating or moving elements were used to average the interference patterns [14]. Wippermann et al. [15] used chirped microlens in a wedge configuration to reduce interference patterns. These two methods can only solve the problem of interference patterns, however, the other two problems are still not solved.

In this paper, we propose a novel beam homogenizer based on random freeform microlenses, called random freeform microlens array (rfMLA). The number of the rfMLA components is minimized and the integration is highly increased. Along with the number reduction, the energy loss caused by the absorption and reflection of the lenses is also reduced. rfMLA is made up of multiple freeform sub-lenses. The rear surface of per sub-lens is a freeform surface, and the front surface is a rectangular. Based on correspondence energy relationship, per freeform surface is designed to achieve a highly uniform homogenized spot on the DMD. Each rectangle is designed to be different and random to break the periodic structure of the MLA, and the purpose of weakening the interference patterns is achieved. The outstanding beam shaping result of the rfMLA has been verified by simulation. The energy efficiency is 69.70%, and the uniformity for incoherent light and coherent light of this novel beam homogenizer are respectively 97.60% and 94.33%.

Although the freeform surfaces was limited due to manufacturing difficulties in the past, 3D printing technology (femtosecond laser direct writing) has developed rapidly, and a wide variety of micro and

* Corresponding author.
E-mail addresses: liuzy_1993@qq.com (Z. Liu), liuhua_rain@aliyun.com (H. Liu).

https://doi.org/10.1016/j.optcom.2019.03.049
Received 1 October 2018; Received in revised form 13 March 2019; Accepted 20 March 2019
Available online 22 March 2019
0030-4018/© 2019 Published by Elsevier B.V.

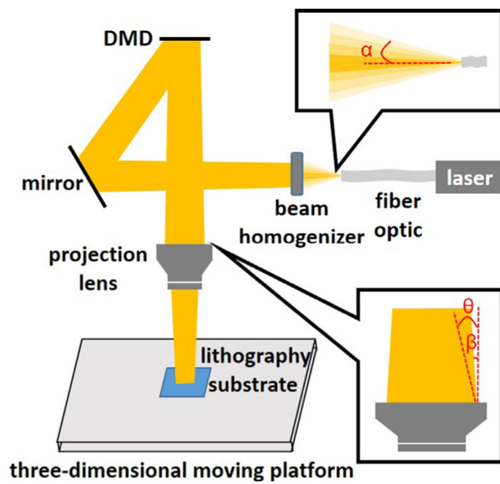

Fig. 1. Schematic diagram of DMD lithography system.

nano optical elements have been successfully demonstrated in recent years [16–20]. As long as the design is reasonable, the freeform surface can be completely processed by the current technology. And this paper only focuses on the design method and the application of freeform surfaces.

2. Principle and methods

DMD lithography system includes the semiconductor laser, the fiber optic, the beam homogenizer, the mirror, the spatial light modulator (DMD), the projection lens and the three-dimensional moving platform, as shown in Fig. 1. The beam from the laser tube is coupled to one end of the fiber optic and emitted from the other end. The beam from the fiber optic can be seen as a point light source with a divergence angle α and a Gaussian intensity distribution. The emitted beam is homogenized by the beam homogenizer and forms a homogenized spot on the DMD. DMD is a rectangle consisting of millions of square micromirrors. Each micromirror controlled by computer has three states "reset", "on" and "off". When DMD is not working, each micromirrors are in the "reset" state. When DMD is working, each micromirrors are in the "on" or "off" state. The micromirror deflects +12° when the micromirror is in the "on" state. The tiny spot on the micromirror will be reflected into the projection lens and image on the lithography substrate. This is equivalent to forming a corresponding tiny bright spot on the lithography substrate. The micromirror deflects −12° when the micromirror is in the "off" state. The tiny spot on the micromirror will be reflected to other positions without entering the projection lens. This is equivalent to forming a corresponding tiny dark spot on the lithography substrate. By the control of each micromirror, different patterns can be formed on the lithography substrate.

2.1. The basic design parameters of fMLA

The divergence angle of the point light source can be expressed:

$$\sin\alpha = NA \tag{1}$$

Here, *NA* is the numerical aperture of the fiber optic.

On the lithography substrate, different energy of each tiny bright spot can result in inconsistent optical resolution of the lithography pattern [9]. In order to obtain a good lithography quality, the following two conditions need to be satisfied:

(i) the uniformity of the homogenized spot on the DMD is usually required to be above 90%;

(ii) each tiny spot reflected by the micromirror can be collected by the projection lens, when in the "on" state.

For the first condition, we use fMLA as a beam homogenizer. For easy analysis, we replace the DMD with its image which is symmetrical about the mirror. The angle between the vertical plane of the homogenizer's optical axis and the DMD (the image of the DMD) is φ. The schematic diagram of the fMLA is shown in Fig. 2. The fMLA is a square consisting of N ∗ N, a total of N^2 sub-lenses. The beam from the light source is split into N^2 sub-beams by the fMLA, and one sub-lens corresponds to one sub-beam. As long as the number of sub-lenses is sufficient, the intensity of each sub-beam is considered to be uniform. The front surface of each sub-lens is a rectangle and the rear surface is a freeform surface. By the design of freeform surfaces, all sub-beams are deflected and eventually superimposed on the DMD so that the uniformity is further improved [21]. The fMLA not only can split the beam, but can also deflect the sub-beams. Thus, Gaussian beams or other types of nonuniform beams can be homogenized with only one fMLA without a collimating lens and a Fourier lens. The side length of the fMLA is given by:

$$P = 2l_1 \tan\alpha \tag{2}$$

Here, l_1 is the distance between the light source and the fMLA. Substituting Eq. (1) into Eq. (2), the side length of the fMLA can be derived as:

$$P = 2l_1\sqrt{\frac{NA^2}{1-NA^2}} \tag{3}$$

The second condition is satisfied, as long as:

$$\gamma < \theta \tag{4}$$

Here, γ is the diffusing angle in diagonal direction for the beam from the DMD, and θ is the largest collection angle of the projection lens. We firstly calculate β the diffusing angle in y direction for the beam from the DMD. Based on the law of reflection, the diffusing angle in y direction for the sub-beam emitted from the top sub-lens is also β, and it is given by:

$$\tan\beta = \frac{P + T_y\cos\varphi}{2l_2 + T_y\sin\varphi} \tag{5}$$

Here, l_2 is the distance between the fMLA and the image of DMD, and T_y is the width of the DMD. Note that the size of one sub-lens is ignored compared with the fMLA.

In Eq. (5), the side length of the fMLA and DMD are respectively replaced by their diagonal lengths, and the diffusing angle in diagonal direction for the beam from the DMD can be given by:

$$\tan\gamma = \frac{P' + T'\cos\varphi}{2l_2 + T'\sin\varphi} \tag{6}$$

With:

$$P' = \sqrt{2}P \tag{7}$$

$$T' = \sqrt{T_x^2 + T_y^2} \tag{8}$$

Here, T_x is the length of the DMD. Substituting Eqs. (3), (7) and (8) into Eq. (6), the diffusing angle in diagonal direction for the beam from the DMD can be derived as:

$$\tan\gamma = \frac{2l_1\sqrt{\frac{2NA^2}{1-NA^2}} + \sqrt{T_x^2+T_y^2}\cos\varphi}{2l_2 + \sqrt{T_x^2+T_y^2}\sin\varphi} \tag{9}$$

2.2. Design method of freeform surface

The light from the point light source is refracted when it passes through the front and back surfaces of the sub-lens and finally illuminates the DMD. Dividing the freeform surface and the image of DMD

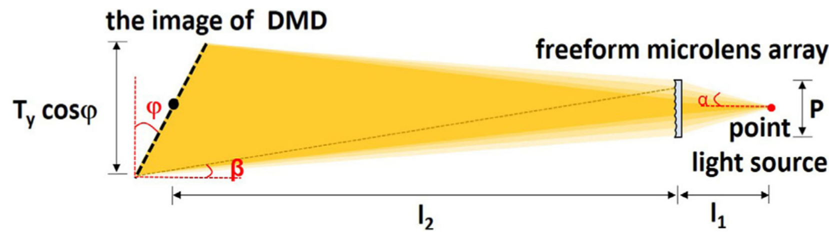

Fig. 2. Schematic diagram of fMLA.

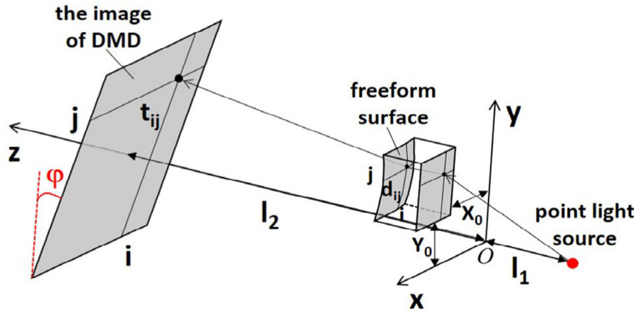

Fig. 3. Schematic of energy grids on the freeform surface and the image of DMD.

equally into M ∗ M a total of M^2 energy grids, as shown in Fig. 3. The energy grids' intersecting coordinate of the ith column and the jth row on the freeform surface can be expressed as $d_{ij}(d_{xi}, d_{yj}, d_{zij})$:

$$d_{xi} = X_0 + \frac{i}{M} d_x \tag{10}$$

$$d_{yj} = Y_0 + \frac{j}{M} d_y \tag{11}$$

$$d_{zij} = z_{ij} \tag{12}$$

Here, X_0 is the distance between the sub-lens and the y-axis, Y_0 is the distance between the sub-lens and the x-axis, d_x is the length of the sub-lens, d_y is the width of the sub-lens, z_{ij} is the height of the freeform surface, $i = 1, 2, 3 \ldots M$, and $j = 1, 2, 3 \ldots M$.

The energy grids' intersecting coordinate of the ith column and the jth row on the image of DMD can be expressed as $t_{ij}(t_{xi}, t_{yj}, t_{zij})$:

$$t_{xi} = \left(\frac{i}{M} - 0.5\right) T_x \tag{13}$$

$$t_{yj} = \left(\frac{j}{M} - 0.5\right) T_y \cos\varphi \tag{14}$$

$$t_{zij} = l_2 - \left(\frac{j}{M} - 0.5\right) T_y \sin\varphi \tag{15}$$

There is a one-to-one correspondence between d_{ij} and t_{ij}. Establish partial differential equations based on the Snell's law and the energy conservation law, and all the energy grids' intersecting coordinates on the freeform surface can be obtained by solving the numerical solution of the partial differential equations. And then the freeform surface can be obtained by fitting all intersecting coordinate into a smooth surface. The shape of freeform surfaces at each locations is different, and Fig. 4 shows one of all freeform surfaces.

2.3. Design method of sub-lens space distribution

According to the distribution patterns of the sub-lenses, fMLA can be classified into two type, one is the periodic freeform microlens array (pfMLA) and the other is irregularly distributed rfMLA.

2.3.1. pfMLA

For sub-lenses which are regularly distributed, the front surface of each sub-lens is designed to be a same square and the rear surface is designed to be a freeform surface. There is a symmetry relationship between every two y-axis symmetric sub-lenses. Therefore, only the sub-lenses on the one side of the y-axis need to be designed. The design model of pfMLA is shown in Fig. 5. (a). The side length of the square is given by:

$$d = \frac{P}{N} \tag{16}$$

2.3.2. rfMLA

For sub-lenses which are irregularly distributed, the front surface of each sub-lens is designed to be a different rectangle and the rear surface is designed to be a freeform surface. There is no symmetry between all sub-lenses, and all sub-lenses need to be designed. The length and the width of each rectangle are respectively satisfied:

$$d_x = d + R \times 0.2d \tag{17}$$

$$d_y = d + R \times 0.2d \tag{18}$$

Here, R is a random value ranged from −1 to 1. The length and width of each sub-lens are different and random ranged from 0.8d to 1.2d. The model of rfMLA is shown in Fig. 5(b).

Table 1
System parameters.

Parameters	Value
Wavelength	405 nm
The numerical aperture of the fiber optic	0.22
The material of the lenses	Silica
The size of the DMD	20.736 mm ∗ 11.664 mm
The largest collection angle of the projection lens	10°
The angle between the vertical plane of the homogenizer's optical axis and the DMD	24°

3. Simulation

The system parameters for designing the beam homogenizer are shown in Table 1. The material of fMLA is silica, which can be processed by femtosecond laser direct writing. Once processed, it can be used as a substrate for bulk copying with UV-cure polymer, and production costs will be greatly reduced. Moreover, the thermal stability of silica is good, it can work in the temperature range of 10–80 degrees, and the applicable laser power density can reach 50 W/cm^2. In order to achieve the desired uniformity, we used 8 ∗ 8 a total 64 sub-lenses. If the optical system has higher uniformity requirements, we could use more sub-lens numbers. The distance between the light source and the fMLA is 10 mm in order to be easy to integrate. Based on Eq. (3), the side length of the fMLA can be calculated as 4.51 mm. So as to obtain a good lithography quality, the diffusing angle in diagonal direction for the beam from the DMD is 8°. According to Eq. (9), the distance between the fMLA and the image of DMD can be obtained to be 88.76 mm.

On the basis of the above-mentioned parameters, the sub-lenses at each position are designed and finally assembled into fMLA, as shown in Fig. 5. tMLA and fMLA are simulated by the optical software ZEMAX, their optical pathway diagrams are shown in Fig. 6.

The irradiance maps of the homogenized spot simulated by three beam homogenizers are shown in Fig. 7. From Fig. 7(b) and (c), it

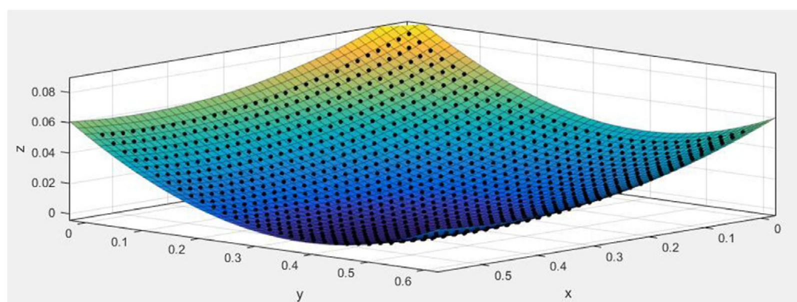

Fig. 4. The design shape of one freeform surface.

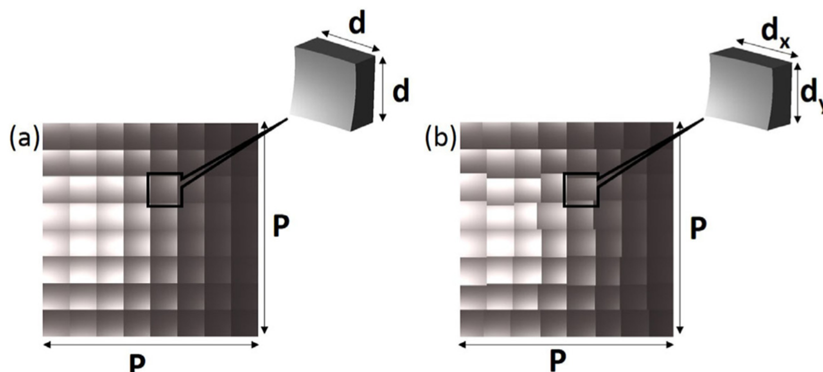

Fig. 5. The design model of (a) pfMLA and (b) rfMLA.

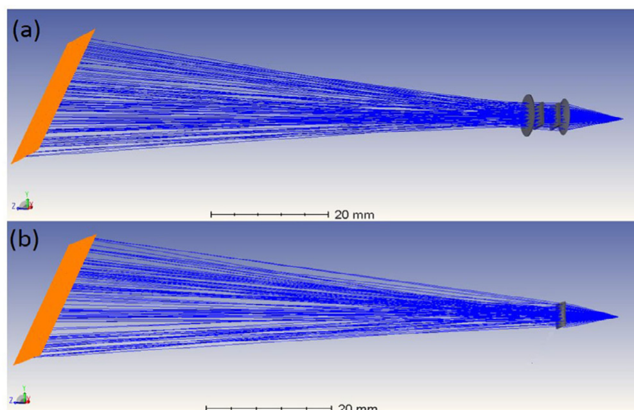

Fig. 6. Optical pathway diagrams of (a) tMLA and (b) fMLA.

can be known that the homogenized spot simulated by the pfMLA and rfMLA has weak energy at the edge position. This is caused by the design errors. The size of the homogenized spot can be designed to be appropriately larger than the size of the DMD, so that DMD can be located at black frame position which is relatively uniform in Fig. 7. From Fig. 7(a), it can be found that the size of the homogenized spot simulated by the tMLA can also be designed to be appropriately enlarged to ensure that the homogenized spot can completely cover the DMD. This is caused by the DMD which is not perpendicular to the homogenizer's optical axis. Obviously, enlarging the spot size will result in some energy loss.

As can be seen from Fig. 7, pfMLA improves the beam shaping result for incoherent light, but the beam shaping result for coherent light is poor. Because pfMLA has serious periodicity, there are still obvious regular interference patterns. However rfMLA significantly improves the beam shaping result for both coherent light and coherent light, and the interference patterns are greatly weaken.

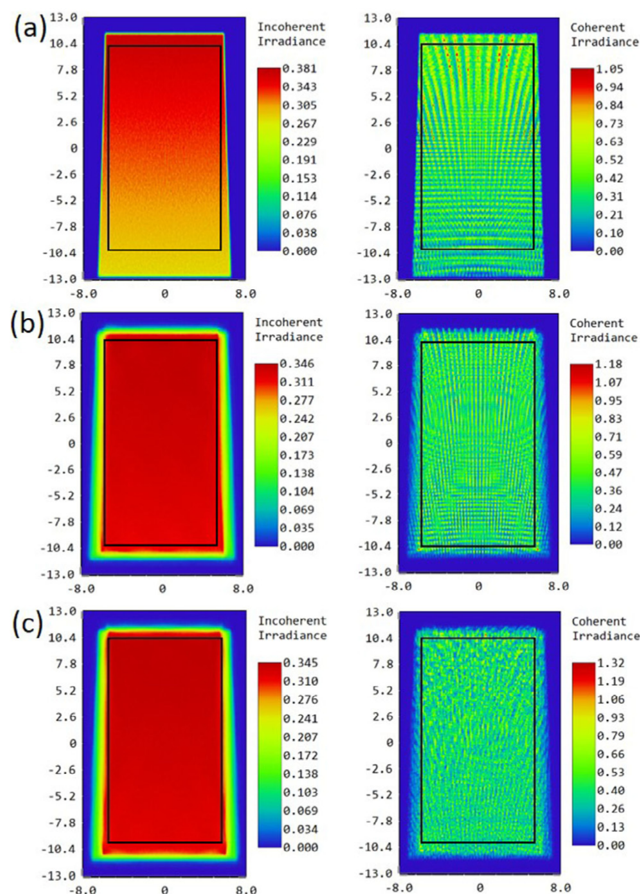

Fig. 7. The irradiance maps on the DMD simulated by (a) tMLA, (b) pfMLA, and (c) rfMLA. The left side is the incoherent irradiance maps. The right side is the coherent irradiance maps.

Table 2
Energy efficiency and uniformity of the homogenized spot.

Homogenizer	Deviation	Energy efficiency	Uniformity for incoherent light	Uniformity for coherent light
tMLA	Nothing	62.00%	91.93%	79.00%
pfMLA	Nothing	69.48%	97.66%	88.77%
rfMLA	Nothing	69.70%	97.60%	94.74%
rfMLA	Decentering 30 μm about x-axis	69.55%	97.36%	94.71%
rfMLA	Decentering 30 μm about y-axis	69.58%	97.41%	94.25%
rfMLA	Decentering 30 μm about z-axis	69.72%	97.60%	94.33%
rfMLA	Tilting 1° about x-axis	69.77%	96.98%	93.32%
rfMLA	Tilting 1° about y-axis	69.83%	97.50%	94.37%
rfMLA	Tilting 1° about z-axis	69.60%	97.56%	93.66%
rfMLA	The wavelength is 380 nm	67.60%	97.66%	94.03%
rfMLA	The wavelength is 520 nm	69.74%	97.41%	93.29%

In order to further quantify the beam shaping result, the image of DMD is divided into multiple units, and the uniformity is defined by:

$$\varepsilon = \left(1 - \sqrt{\frac{\sum_{i=1}^{n}\left(E_i - \bar{E}\right)^2}{n\bar{E}^2}}\right) \times 100\%, \quad (19)$$

Here, n is the number of units, E_i is the irradiance of each unit, and $\bar{E}$ is the mean value of all E_i.

Considering the Fresnel loss, the MLA is not coated and the transmittance is 92%. Other lenses are coated with an anti-reflection film and the transmittance are 98%. The energy efficiency and uniformity of the homogenized spot simulated by three beam homogenizers are show in Table 2.

Limited by the precision of the mobile platform and some unavoidable operational errors, the real position of the homogenizer will deviate from the ideal position, and this will cause an adverse effect for the beam shaping result. Table 2 also shows the energy efficiency and uniformity of homogenized spot for tilting rfMLA 1° about the x-axis, y-axis, and z-axis respectively or decentering rfMLA 30 μm about the x-axis, y-axis, and z-axis respectively. This assembling tolerance can be achieved completely by the mechanical structure. And fMLA is a refractive homogenizer, which is not very sensitive to wavelengths like the diffractive element. Its suitable wavelength range is relatively large. It has a good beam shaping result in the wavelength range of 380–520 nm.

One thing to note is that the specific fMLA is usually not suitable for other optical systems. Of course, according to different correspondence energy relationship, an arbitrary shape of the homogenized spot can be designed.

4. Conclusions

We report a novel beam homogenizer for DMD lithography system. It exhibits a good optical performance. Compared with the tMLA, the energy efficiency and the uniformity for incoherent light and coherent light have been improved from 62.00% to 69.70%, from 91.93% to 97.60%, and from 79.00% to 94.33%, respectively. It is worth noting that the novel beam homogenizer has only one component, and the distance between the light source and the fMLA can be designed to be very short. This provides great convenience for integration. In production, the beam homogenizer can be made into a "hat" by 3D printing technology and worn directly on the fiber optic in the future. Our research provides a feasible way for the integration of DMD lithography system and other optical systems, which has great practical value.

Acknowledgments

The work described in this paper is supported by the National Natural Science Foundation of China under grant No. 61875036, Projects of Science and Technology Development Plan of Jilin Province (20190302049GX), the State Key Laboratory of Applied Optics, and the Lab of Space Optoelectronic Measurement.& Perception (LabSOMP-2018-05).

References

[1] P. Hahmann, O. Fortagne, 50 years of electron beam lithography: Contributions from jena (Germany), Microelectron. Eng. 86 (2009) 438–441.
[2] R. Kaesmaie, H. Loschner, Ion projection lithography: Progress of European MEDEA & international program, Microelectron. Eng. 53 (2000) 37–45.
[3] S.R.J. Brueck, Optical and interferometric lithography - nanotechnology enablers, Proc. IEEE 93 (2005) 1705–1721.
[4] K.F. Chan, Z. Feng, R. Yang, A. Ishikawa, W. Mei, High-resolution maskless lithography, J. Micro-Nanolith Mem. 2 (2003) 331–339.
[5] R. H.Chen, H. Liu, H.L. Zhang, Edge smoothness enhancement in DMD scanning lithography system based on a wobulation technique, Opt. Express. 25 (2017) 21958–21968.
[6] D.J. Heath, J. Grant-Jacob, R.W. Eason, Single-pulse ablation of multi-depth structures via spatially filtered binary intensity masks, Appl. Opt. 57 (2018) 1904–1909.
[7] Q.K. Li, Y. Xiao, H. Liu, H.L. Hao, W.J. Zhang, J. Xu, J.H. Li, Analysis and correction of the distortion error in a DMD based scanning lithography system, Opt. Commun.
[8] S.Z. Huang, M.J. Li, L.G. shen, Flexible fabrication of biomimetic compound eye array via two-step thermal reflow of simply pre-modeled hierarchic microstructures, Opt. Commun. 293 (2017) 213–218.
[9] Z. Xiong, H. Liu, R.H. Chen, J. Xu, Q.K. Li, J.H. Li, W.J. Zhang, Illumination uniformity improvement in digital micromirror device based scanning photolithography system, Opt. Express. 26 (2018) 18597–18607.
[10] S. Pfadler, F. Beyrau, M. Loffler, A.Leipertz, Application of a beam homogenizer to planar laser diagnostics, Opt. Express. 14 (2006) 10171–10180.
[11] P.H. Yao, C.H. Chen, C.H. Chen, Low speckle laser illuminated projection system with a vibrating diffractive beam shaper, Opt. Express. 20 (2012) 16552–16566.
[12] Y.Y. Li, C.K. Qiu, P. Li, T.W. Xing, W.M. Lin, C.X. Zhou, Shape the unstable laser beam using diffractive optical element array, Proc. SPIE. 7848 (2010) 78481X.
[13] R. Sundar, K. Ranganathan, S.M. Oak, Generation of flattened Gaussian beam profiles in a Nd: YAG laser with a Gaussian mirror resonator, Appl. Opt. 47 (2008) 147–152.
[14] R. Voelkel, K.J. Weible, Laser beam homogenizing: Limitations and constraints, Proc. SPIE 7102 (2008) 71020J.
[15] F. Wippermann, U.D. Zeitner, P. Dannberg, A. Bräuer, S. Sinzinger, Beam homogenizers based on chirped microlens arrays, Opt. Express. 15 (2007) 6218–6231.
[16] T. Gissibl, S. Thiele, A. Herkommer, H. Giessen, Two-photon direct laser writing of ultracompact multi-lens objectives, Nat. Photonics 10 (2016) 554–560.
[17] T. Gissibl, S. Thiele, A. Herkommer, H. Giessen, Sub-micrometre accurate free-form optics by three-dimensional printing on single-mode fibres, Nat. Commun. 7 (2016) 11763.
[18] S. Thiele, T. Gissibl, H. Giessen, A. Herkommer, Ultra-compact on-chip LED collimation optics by 3D femtosecond direct laser writing, Opt. Lett. 41 (2016) 3029–3033.
[19] F. Kotz, K. Arnold, W. Bauer, D. Schild, N. Keller, K. Sachsenheimer, T.M. Nargang, C. Richter, D. Helmer, B.E. Rapp, Three-dimensional printing of transparent fused silica glass, Nature 544 (2017) 337–340.
[20] B. Hao, H.W. Liu, F. Chen, Q. Yang, P.B. Qu, G.Q. Du, J.H. Si, X.H. Wang, X. Hou, Versatile route to gapless microlens arrays using laser-tunable wet-etched curved surfac, Opt. Express. 20 (2012) 12939–12948.
[21] H. Urey, K.D. Powell, Microlens-array-based exit-pupil expander for full-color displays, Appl. Opt. 44 (2005) 4930–4936.